CHARACTERISTICS OF THE SL100 — A NEW COMMERCIAL NEODYMIUM LASER GLASS

By W. Ryba-Romanowski and B. Jeżowska-Trzebiatowska

Institute for Low Temperature and Structure Research, Polish Academy of Sciences, Wrocław*

(Received December 1, 1977)

Systematic studies of laser properties of a new commercially available SL100 laser glass were performed using the theory developed by Judd and Ofelt and the experimental data. The laser glass showed relatively low threshold for laser action and stability of the spectroscopic and optical properties. The obtained results were compared with the published data on the other commercial silicate glasses.

1. Introduction

Since first demonstration of laser action in a neodymium-doped glass in 1961 [1], considerable progress has been made in developing the laser glasses for specific applications, as for example room temperature CW lasers, or large aperture disk amplifiers.

Also large Nd: glass laser systems were designed for fusion applications [2]. Up to now however, there exist very few manufacturers of good quality laser glass. That is why every new commercially available laser glass attracts the attention of the actual and potential users of this material.

In this work, we present the relevant characteristics of the commercial neodymium doped silicate laser glass developed in our country[1].

The emission properties of laser glass were studied on the basis of the theory for crystal-field-induced electric dipole transitions between $4f$ states of the rare earth ions developed by Judd [3] and Ofelt [4]. This theory has been successfully applied to the analysis of laser properties of the rare earth doped crystals, glasses and liquids [5–7]. This theory permits relatively rapid determination of the emission properties of particular laser material, and what is more important, offers the possibility of comparison of laser materials studied in different laboratories.

---

* Address: Instytut Niskich Temperatur i Badań Strukturalnych PAN, P.O. Box 937, 50-950 Wrocław, Poland.

[1] This work is a result of cooperation of Institute for Low Temperature and Structure Research, Polish Academy of Sciences and the Jelenia Góra Optical Works, devoted to the design and development of the rare earth doped laser glasses.

2. Theoretical background

In this Section we present the relevant aspects of the Judd and Ofelt theory.

The oscillator strength P of an electric dipole transition between initial $|4f^n[S, L]J\rangle$ level and terminal $|4f^n[S, 'L']J\rangle$ level of the rare earth ion is given by

$$P = \frac{8\pi^2 mc}{3h(2J+1)\lambda} \frac{(n^2+9)^2}{9n} \sum_t \Omega_t |\langle |4f^n[S, L]J \| U^t \| [S'L']J' \rangle|^2, \tag{1}$$

where λ is the mean wavelength of the transition, n is material's index of refraction at the mean wavelength of the transition, $\langle ||U^t|| \rangle$ are the doubly reduced unit tensor operators calculated in the intermediate coupling approximation. The three coefficients Ω_2, Ω_4 and Ω_6 contain implicitly the odd crystal field terms, radial integrals, and perturbation energy denominators. These quantities are regarded as the empirical parameters, which are determined by a least squares fit between the oscillator strengths measured in the absorption spectrum, and calculated using Eq. (1).

Similarly, the spontaneous emission probability A for an electric dipole transition between excited level $|4f^n[S, L]J\rangle$ and lower lying level $|4f^n[S'L']J'\rangle$ is

$$A = \frac{64\pi^2 e^2 n^2}{3h(2J+1)\lambda^3} \frac{(n^2+2)^2}{9n} \sum_t \Omega_t |\langle 4f^n[S, L]J \| U^t \| 4f^n[S'L']J' \rangle|^2. \tag{2}$$

Sum of the transition probabilities from initial excited level to all lower lying levels is defined as the total radiative transition probability A_{tot} from initial excited level

$$A_{\text{tot}} = \sum_i A_i \tag{3}$$

and its reciprocal gives the radiative lifetime τ_{rad}

$$\tau_{\text{rad}} = \frac{1}{\sum_i A_i}. \tag{4}$$

The fluorescence branching ratio β and the quantum efficiency η of an excited level are given by

$$\beta = \frac{A_{i-j}}{\sum_j A_{i-j}}, \tag{5}$$

where the summation is made over all possible states of lower energy and

$$\eta = \frac{\tau_{\text{fl}}}{\tau_{\text{rad}}}, \tag{6}$$

where τ_{fl} is measured lifetime of the excited level and τ_{rad} is the calculated radiative lifetime.

The peak induced emission cross section σ_p for the fluorescence transition is related to the radiative transition probability A

$$\sigma_p = \frac{\lambda_p}{8\pi c n^2 \Delta\nu_{eff}} A, \tag{7}$$

where λ_p is the wavelength of the fluorescence peak, and $\Delta\nu_{eff}$ is the effective fluorescence linewidth determined by integrating the fluorescence line shape and dividing by the intensity at λ_p [8].

3. Experimental procedure

The composition of the SL100 laser glass is as follows: 56.6 wt % SiO_2, 24.0 wt % BaO, 14.4 wt % K_2O, 0.9 wt % Sb_2O_3 and 3.0 wt % Nd_2O_3. The nominal Nd_2O_3 concentrations were checked by chemical analysis. From the laser glass the cylindrical rods 160 mm long, 10 mm in diameter were cut, the faces of which were ground and polished to 0.1 μm. From the same glass the $5 \times 20 \times 30$ mm samples were cut, polished and used for spectroscopic measurements.

The absorption spectra were measured with a Cary 14 spectrophotometer, and the fluorescence spectra were measured with a spectrophotometer constructed in our laboratory using a Carl Zeiss GDM1000 monochromator and a phase sensitive detection system. The fluorescence was excited by a HBO-200 high pressure mercury lamp and detected by a photomultiplier with S-1 response, or in the infrared by a cooled PbS detector. The whole detection system was calibrated for spectral response. The fluorescence lifetimes were measured with a TRW Model 75A Decay Time Fluorometer. The uncertainties in the presented values of λ_p, τ_f and $\Delta\nu_{eff}$ are estimated to be no greater than ± 1 nm, $\pm 5\%$ and ± 10 cm^{-1} respectively.

In laser experiments, the laser rod and two exciting linear xenon flashlamps having 160 mm arc length were closely wrapped with an aluminium foil. The flashlamps were energized from a 400 μF condenser bank which could be charged to 2.5 kV. The output energy was measured with a MEL-1 energy meter, and monitored by a photomultiplier connected to an oscilloscope. Resonator consisted of two plane parallel dielectric mirrors with reflectivities of 99.9% and 70.0% spaced by 500 mm.

4. Results

The complete absorption spectrum of the SL100 laser glass with 3 wt % Nd_2O_3 doping is presented in Fig. 1. Extremely strong absorption band at 574 nm corresponding to the $^4I_{9/2} \rightarrow {}^4G_{5/2}, {}^2G_{7/2}$ transition of Nd^{+3} should be noted.

The calculation of absolute radiative transition probabilities from the absorption spectrum require the knowledge of Nd^{+3} ions density in the sample. The Nd^{+3} ions density was determined from the specific weight of the glass and the weight percentage of Nd in the glass. Since the glass was doped with a Nd_2O_3 concentration of 3 wt %, corresponding Nd^{+3} ions density was equal to 2.8×10^{20} cm^{-3}.

The oscillator strengths for transitions from the ground $^4I_{9/2}$ level to excited levels of Nd^{+3} were obtained by numerical integration of nine absorption bands presented in Fig. 1.

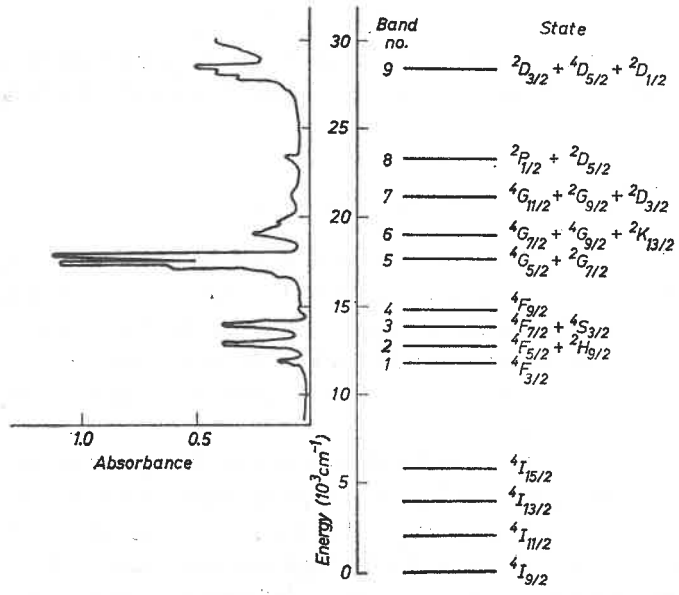

Fig. 1. Absorption spectrum and $4f^3$ electronic energy levels of Nd^{+3} ions in SL100 laser glass. Energy levels are labelled in the Russel-Saunders approximation

The calculated, using Eq. (1), oscillator strengths were next fitted to the measured oscillator strengths by a least squares method. The results of calculation are shown in Table I. The resulting Ω parameters are presented in Table II.

TABLE I

Measured and calculated oscillator strengths for SL100 laser glass

Band number	$\bar{\lambda}$ (μm)	$P(10^{-6})$	
		measured	calculated
1	0.88	0.66	0.85
2	0.81	2.45	2.45
3	0.75	2.17	2.29
4	0.68	0.63	0.18
5	0.58	10.74	10.77
6	0.53	2.68	2.29
7	0.47	0.53	0.44
8	0.43	0.19	0.22
9	0.35	4.58	4.63

For comparative purposes, the Ω parameters for 3669A — American Optical Co., and Ed-2 — Owens Illinois commercial silicate glasses, are also presented in Table II.

The calculated radiative transition probabilities A, resulting radiative lifetimes τ_{rad} and fluorescence branching ratios β_c for SL100 laser glass are shown in Table III. The fluorescence branching ratios β_m obtained by integration of the fluorescence lines are

TABLE II

Ω parameters for SL100, 3669A and ED-2 laser glasses

Parameter	SL100	3669A	ED-2
$\Omega_2(10^{-20}\ cm^2)$	3.09	3.84	3.30
$\Omega_4(10^{-20}\ cm^2)$	1.78	1.95	4.86
$\Omega_6(10^{-20}\ cm^2)$	1.59	1.76	5.18
% rms error	3.1	5.8	3.9

Note: Ω parameters for 3669A and ED-2 laser glasses were taken from [6].

TABLE III

Radiative transition probabilities A, corresponding radiative lifetimes τ_{rad} and fluorescence branching ratios β for SL100 laser glass

Transition	$\bar{\lambda}$ (μm)	A [s^{-1}]	τ_{rad} (μs)	β_c	β_m
$^4F_{3/2} - {}^4I_{9/2}$	0.88	441	2267	0.45	0.47
$- {}^4I_{11/2}$	1.06	456	2192	0.46	0.42
$- {}^4I_{13/2}$	1.35	83	12048	0.08	0.05
$- {}^4I_{15/2}$	1.88	4	250000	0.004	—

also included in this Table. Discrepancies between β_c and β_m values may be due to some uncertainties in calibration of the detection system.

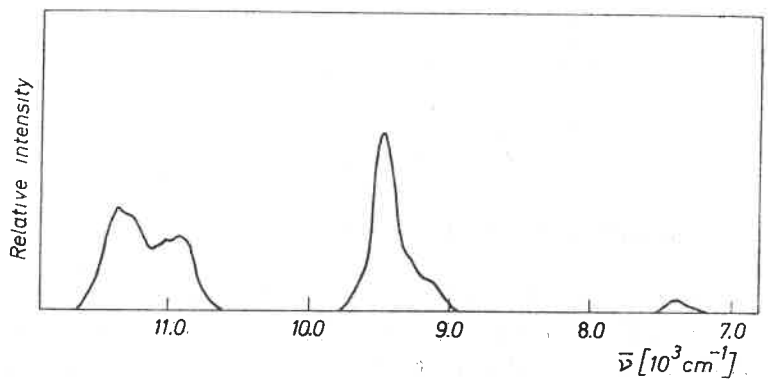

Fig. 2. The complete fluorescence spectrum of Nd^{+3} in SL100 laser glass. Nd_2O_3 doping equal to 3 wt %

The room temperature fluorescence spectrum (Fig. 2) and the results presented above were used for evaluation of the emission properties of the laser glass. These properties are compared with the published data on 3669A and ED-2 glasses in Table IV.

TABLE IV

Emission properties of SL100, 3669A and ED-2 laser glasses

Property	SL100	3669A	ED-2
Radiative lifetime τ_{rad} (μs)	1016	1000	372
Fluorescent lifetime τ_{fl} (μs)	520	520	310
Quantum efficiency η	0.51	0.52	0.83
Effective linewidth at 1.06 μm $\Delta\nu_{eff}$ (cm^{-1})	294	296	300
Effective linewidth at 1.35 μm $\Delta\nu_{eff}$ (cm^{-1})	292	300	366
Peak emission cros section at 1.06 μm σ_p (10^{-20} cm^2)	1.0	1.2	2.9
Peak emission cross section at 1.35 μm σ_p (10^{-20} cm^2)	0.3	0.3	0.7

Note: Emission properties of 3669A and ED-2 laser glasses were taken from [6] and [9].

Several laser rods were tested using the apparatus described in experimental section. No distinct variations of the optical quality of particular rods were observed.

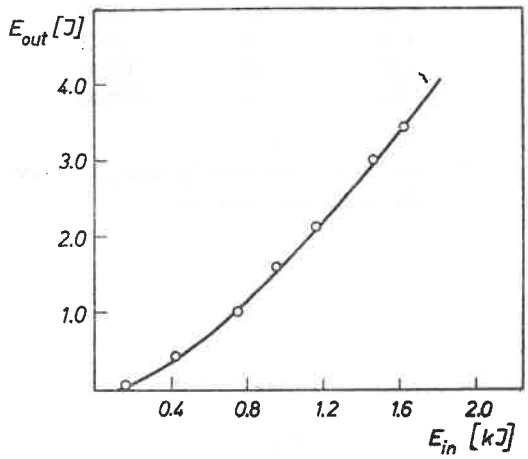

Fig. 3. Input-output characteristics of Nd: glass laser. 30% output mirror

The input-output characteristics of Nd: glass laser studied are presented in Fig. 3. The experimental conditions were as follows: flash time at 1/6 intensity points — 420 μs, resonator length — 500 mm, 30% output mirror. In this configuration the threshold pumping energy was equal to 180 J.

5. Conclusions

On the basis of the Judd-Ofelt theory all relevant characteristics of commercial SL100 laser glass were determined. The accuracy of presented values depend on uncertainties in the evaluation of three Ω parameters and in this study is within $\pm 10\%$.

Although the induced emission cross section for laser transition and the fluorescent quantum efficiency determined are slightly lower than the corresponding values for 3669A laser glass, the low cost and the facility of ordering are the great advantages of SL100 laser glass.

REFERENCES

[1] E. Snitzer, *Phys. Rev. Lett.* **7**, 444 (1961).
[2] *Laser Fusion Annual Report 1974*, UCRL-500-74, Lawrence Livermore Laboratory.
[3] B. R. Judd, *Phys. Rev.* **127**, 750 (1962).
[4] G. S. Ofelt, *J. Chem. Phys.* **37**, 511 (1962).
[5] W. F. Krupke, *IEEE J. Quantum Electron.* **QE-7**, 153 (1971).
[6] W. F. Krupke, *IEEE J. Quantum Electron.* **QE-10**, 450 (1974).
[7] B. Jeżowska-Trzebiatowska, W. Ryba-Romanowski, Z. Mazurak, K. Bukietyńska, *Chem. Phys. Lett.* **43**, 417 (1976).
[8] P. H. Sarkies, J. N. Sandoe, S. Parke, *J. Phys. D* **4**, 1642 (1971).
[9] R. R. Jacobs, M. J. Weber, *IEEE J. Quantum Electron.* **QE-11**, 846 (1975).